

# A Microphysically Inspired Approach to Dark Matter–Dark Energy Interactions: First bounds on dark-sector scattering cross sections.

A.A. Escobal,<sup>1,2,\*</sup> F.B. Abdalla<sup>1,2,†</sup> J.F. Jesus<sup>3,4</sup>, E. Abdalla<sup>5,7,8</sup>, C. Feng<sup>1,2</sup>, and J. A. S. Lima<sup>6</sup>

<sup>1</sup> Department of Astronomy, University of Science and Technology of China, Hefei, Anhui 230026, China.

<sup>2</sup> School of Astronomy and Space Science, University of Science and Technology of China, Hefei, Anhui 230026, China.

<sup>3</sup>Department of Science and Technology, Universidade Estadual Paulista (UNESP),

Instituto de Ciências e Engenharia, Itapeva, SP, 18409-010, Brazil.

<sup>4</sup>Department of Physics, Universidade Estadual Paulista (UNESP),

Faculdade de Engenharia e Ciências de Guaratinguetá, Guaratinguetá, SP, 12516-410, Brazil.

<sup>5</sup>Department of Physics, Universidade de São Paulo, 05508-900, São Paulo, SP, Brazil.

<sup>6</sup>Department of Astronomy, Universidade de São Paulo, 05508-900, São Paulo, SP, Brazil.

<sup>7</sup>Department of Physics, Center for Exact and Natural Sciences,

Federal University of Paraíba, 58059-970, João Pessoa, Brazil

<sup>8</sup>Paraíba State University, 351 Baraúnas Street, University District, Campina Grande, Brazil

(Dated: January 12, 2026)

The observational tension regarding the value of the Hubble constant ( $H_0$ ) has motivated the exploration of alternative cosmological scenarios, including Interacting Dark Energy models. However, the majority of IDE models studied in the literature rely on phenomenological interaction terms proportional to the Hubble parameter (e.g.,  $Q \propto H\rho$ ), which lack a clear microphysical justification and often suffer from large-scale instabilities. In this work, we propose and investigate a “bottom-up” IDE model where the interaction is formulated directly from particle physics collision processes, taking the form  $Q \propto \rho^2$ . This interaction represents a reversible annihilation/creation process between Dark Matter and Dark Energy, motivated by the Boltzmann equation. We test this model against a combination of background cosmological data, including Type Ia Supernovae (Pantheon Plus), Cosmic Chronometers, Baryon Acoustic Oscillations (DESI DR2), and CMB distance priors from Planck18. We find that the model is consistent with the data, yielding a Hubble constant of  $H_0 = 67.71 \pm 0.65 \text{ km s}^{-1} \text{ Mpc}^{-1}$  for the combined analysis. The dimensionless interaction rate coefficients are constrained to be small, with upper limits of  $A < 7.586 \times 10^{-25}$  (for Dark Matter self annihilation) and  $B < 0.048$  (for Dark Energy self annihilation) at 95% confidence level. Since the interaction model is parameterized by the expansion rate, these bounds on  $H_0$ ,  $A$ , and  $B$  directly translate into a strict limit on the thermally-averaged annihilation cross-section per unit of mass. The constraints on the coupling  $A$  imply that, if such a collisional interaction exists, the effective dark-matter annihilation cross section per unit mass is highly suppressed relative to the cosmological expansion rate. In contrast, the corresponding dark-energy contribution, governed by  $B$ , is only constrained at the level of a few percent in dimensionless units.

## I. INTRODUCTION

Currently, the best description of observed cosmology is given by the flat  $\Lambda$  Cold Dark Matter model ( $\Lambda$ CDM-flat). While it successfully describes most astronomical observations, both from the early Universe, such as primordial nucleosynthesis data [1] and the Cosmic Microwave Background (CMB) [2], and from the late Universe, such as measurements of Type Ia supernovae (SNe Ia) [3] and Hubble parameter data,  $H(z)$  [4], it faces several critical challenges [5]. The most pressing of these is the so-called  $H_0$  tension [6, 7], a statistically significant discrepancy around ( $\sim 4 - 6\sigma$ ) between the value of the Hubble constant measured from early Universe probes and that measured by local late Universe observation probes.

The current statistical tensions, along with other issues within the standard model, present an opportunity

to explore alternative models that may arise from modifications in gravitational theory or changes in the matter-energy content composing the dark sector. By maintaining General Relativity and altering the material content, we consider models with interaction between dark energy and dark matter, known as interacting dark energy (IDE) models. The possibility of interaction between dark energy and dark matter is an intriguing avenue for studying the dark sector of the Universe as well as implications within particle physics. IDE cosmological models have been extensively discussed in the literature [7–31]. Considering possible couplings between these unknown components, energy transfer may occur from dark energy to dark matter or vice versa. More generally, both processes may operate simultaneously, leading to a bidirectional exchange within the dark sector.

IDE models are natural candidates for addressing the Coincidence Problem, as the ratio of the dark sector components is dynamic. Recently, IDE models have been extensively applied to address the  $H_0$  problem [7, 21, 25, 27, 28]. However, the vast majority of IDE models explored in the literature are “top-down” phe-

\* Contact author: anderson.aescobal@outlook.com

† Contact author: filipe.abdalla@gmail.com

nomenological *ansatzes* [15, 18, 21–23, 27–30]. The most common forms, such as terms proportional to the Hubble function times the energy density of some material component (e.g.,  $Q \propto H\rho$ ), are motivated by dimensional analysis rather than a fundamental microphysical theory. This popular approach faces significant theoretical challenges: it relies on a “non-local” interaction dependent on the global expansion rate ( $H$ ) and, as demonstrated in [32, 33], can suffer from catastrophic large-scale instabilities in the early universe. While some authors [34, 35] have considered a non-linear interaction term  $Q \propto H\rho^2$ , no justification based on first principles has been presented.

In contrast, this work explores a “bottom-up” model. Based on the particle physics framework of equilibrium processes [36], we propose and investigate an interaction term  $Q$  formulated directly from the microphysics of local particle collisions. This term represents a reversible collision process at the field level,  $\chi + \chi \longleftrightarrow \phi + \phi$ , where  $\chi$  represents the dark matter field and  $\phi$  the Dark energy field, corresponding to local, number changing interactions within the dark sector. As an effective description grounded in microphysics, this formulation is theoretically well defined and more physically grounded than the common interaction terms of the form  $Q \propto H\rho$ .

The primary goal of this paper is to test this new, microphysically-motivated IDE model against cosmological observations. We explore its capacity to alleviate the  $H_0$  tension by performing a statistical analysis to obtain observational constraints on its parameters, particularly the interaction coefficients. For this, we use a combined dataset of Cosmic Chronometers (CCs) [4], Type Ia Supernovae (SNe Ia) from Pantheon Plus [3], more recent measurements of Baryon Acoustic Oscillations (BAO) from DESI DR2 [37], and distance priors from the CMB [38].

The article is organized as follows. In Section II, we begin with the presentation of the dynamic formulation of interacting models. In Section III we motivate our interaction term from a Lagrangean point of view and specify which types of dark matter and dark energy can be assumed to match our model. Section IV discusses the observational data sample used and the statistical methods applied in our analyses. In Section V, we present the results obtained, and finally, in Section VI, we present our conclusions and discuss future perspectives of our work.

## II. DYNAMIC FORMULATION OF THE IDE MODEL

To evaluate the interaction between dark matter and dark energy, we postulate an interaction term  $Q_i^\nu$ . The non-conservation of the energy-momentum tensor for these individual components is thus

$$\nabla_\mu T_i^{\mu\nu} = Q_i^\nu. \quad (1)$$

Considering the interaction 4-vector  $Q_i^\nu = [Q_i/a, 0, 0, 0]^T$ , as implemented in [15], and defining  $Q_{\text{DM}} = Q = -Q_{\text{DE}}$  within the context of the FLRW metric, the background-level conservation laws for the dark matter ( $\bar{\rho}_{\text{DM}}$ ) and dark energy ( $\bar{\rho}_{\text{DE}}$ ) densities are:

$$\dot{\bar{\rho}}_{\text{DM}} + 3H\bar{\rho}_{\text{DM}} = \frac{Q}{a}, \quad (2)$$

$$\dot{\bar{\rho}}_{\text{DE}} + 3H\bar{\rho}_{\text{DE}}(1+w) = -\frac{Q}{a}. \quad (3)$$

Here, the overdot denotes the derivative with respect to cosmic time,  $a$  is the scale factor,  $w$  is the dark energy equation of state parameter, and  $H$  is the Hubble parameter. We have  $Q > 0$  when dark energy is changing into dark matter, while  $Q < 0$  corresponds to DM changing into DE. Baryons and radiation are assumed to be conserved separately and evolve as in the standard  $\Lambda$ CDM model.

To explore new routes with interaction models in the dark sector in search of addressing the  $H_0$  tension, in this work we propose and analyze an interaction term that differs from the models commonly proposed in the literature. The most widely-used forms, such as terms linear in the energy density and proportional to the Hubble parameter (e.g.,  $Q \propto H\bar{\rho}$ ) [9, 15, 32, 33], are largely phenomenological *ansatzes*. Their motivation stems primarily from dimensional analysis (as  $H \times \bar{\rho}$  has the correct physical units of Energy Density/Time) and mathematical simplicity, rather than a first-principles microphysical theory.

This popular *ansatz* faces significant theoretical challenges: it relies on a “non-local” interaction that depends on the global expansion rate ( $H$ ) rather than on local fluid properties. Furthermore, as discussed in [32, 33], many of these models suffer from catastrophic large-scale instabilities in the early universe, which can render them non-viable. The physical motivation for this  $Q \propto \bar{\rho}^2$  form is motivated by analogy to the standard Boltzmann collision term for particle annihilation discussed in Chapter 5 of [36]. In a typical particle physics scenario, such as the annihilation of a generic particle  $\psi$ , the evolution of its number density  $n_\psi$  is given by [36, Eq. 5.24]:

$$\frac{dn_\psi}{dt} + 3Hn_\psi = -\langle\sigma|v|\rangle \left[ n_\psi^2 - (n_\psi^{EQ})^2 \right] \quad (4)$$

where  $\langle\sigma|v|\rangle$  is the thermally-averaged annihilation cross-section, and the terms  $-\langle\sigma|v|\rangle n_\psi^2$  and  $+\langle\sigma|v|\rangle (n_\psi^{EQ})^2$  represent the annihilation and creation processes, respectively. By substituting the mass density  $\bar{\rho} = mn$  for non-relativistic particles, the collision term in Eq. (4) takes the form:

$$\dot{\bar{\rho}}_\psi + 3H\bar{\rho}_\psi = -\frac{\langle\sigma|v|\rangle}{m_\psi} \bar{\rho}_\psi^2 + \frac{\langle\sigma|v|\rangle}{m_\psi} (\bar{\rho}_\psi^{EQ})^2 \quad (5)$$

In contrast, this work explores a “bottom-up” model. Our proposed interaction term  $Q$  is formulated directly

from the microphysics of local particle collisions, by applying Eq. (4) to dark matter and dark energy, we obtain the interaction term:

$$Q = -A \frac{H_0}{\bar{\rho}_{c,0}} \bar{\rho}_{\text{DM}}^2 + B \frac{H_0}{\bar{\rho}_{c,0}} \bar{\rho}_{\text{DE}}^2. \quad (6)$$

Here,  $A$  and  $B$  are the dimensionless and positive interaction rate coefficients. The term  $\bar{\rho}_{c,0}$  represents the critical energy density at the present epoch. The term  $Q$  models the interaction between dark matter and dark energy as a reversible collision process; specifically, the full interaction term  $Q$  represents the net balance of this reaction. The sign of  $Q$ , and thus the net direction of energy flow, depends on the dynamical competition between these two processes throughout cosmic history.

### III. EFFECTIVE FIELD-THEORY INTERPRETATION OF THE DARK-SECTOR INTERACTION

At the microscopic level, the interaction considered in this work can be interpreted within an effective field theory framework involving two dark-sector fields, denoted by  $\chi$  and  $\phi$ , associated with dark matter and dark energy, respectively. For bosonic dark matter, a minimal and renormalizable realization of the interaction is provided by quartic operators in the Lagrangian density. In the case of scalar dark matter [39], this takes the form  $\mathcal{L}_{\text{int}} \propto \chi^2 \phi^2$ , while for vector dark matter one may write  $\mathcal{L}_{\text{int}} \propto (\chi_\mu \chi^\mu) \phi^2$ . Both interactions are Lorentz invariant, local, and renormalizable, and mediate reversible  $2 \rightarrow 2$  processes of the type  $\chi + \chi \leftrightarrow \phi + \phi$ . For Majorana fermionic dark matter, an analogous interaction can arise from  $\mathcal{L}_{\text{int}} \sim (\bar{\chi} \chi) \phi^2 / \Lambda_c$ , where  $\Lambda_c$  is an energy cutoff scale, possibly related to the Dark Sector particle. Further possibilities may include derivatives in the effective Lagrangian description. This operator leads to the same quadratic dependence of the interaction term at the coarse-grained, background level. Axion or axion-like dark matter [40] may also be accommodated within this framework, with the important caveat that couplings such as  $a^2 \phi^2$  are forbidden given the axion-like symmetry properties. In this case, an interaction can arise only through breaking of this shift symmetry.

For this interaction to be operative, the dark matter field  $\chi$  must admit number-changing self-annihilation processes. This requirement naturally selects  $\chi$  to be a bosonic field, such as a scalar or vector degree of freedom, or a Majorana fermion. In particular, standard fermionic dark matter would require additional internal quantum numbers or higher-dimensional operators to allow for  $\chi \chi$  annihilation without violating Fermi statistics.

The dark energy component  $\phi$  is assumed to be a dynamical field rather than a strict cosmological constant. This assumption is essential, as a vacuum energy term does not support particle-like excitations or number-changing interactions. In this framework,  $\phi$  may be interpreted as a light scalar field or condensate, capable of

participating in local interactions while maintaining an effective equation of state close to  $w \simeq -1$  at the background level. The interaction considered here therefore excludes models in which dark energy is exactly constant or purely geometric in origin.

It is important to emphasize that not all dark-sector interactions are compatible with the present framework. Linear decay channels, such as  $\chi \rightarrow \phi$  or  $\phi \rightarrow \chi$ , are explicitly excluded by this  $Q$  interaction and other forms of  $Q$  must be used, as they would lead to qualitatively different phenomenology. Likewise, interaction terms proportional to a single power of the energy density do not arise from local  $2 \rightarrow 2$  processes and are not supported by this effective field theory interpretation. The quadratic dependence of the interaction term thus reflects the underlying assumption that energy exchange in the dark sector is dominated by local, two-particle collisions.

Within these assumptions, Eq. (6) should be interpreted as the coarse-grained, background-level manifestation of an underlying microphysical interaction, analogous to the annihilation and creation terms familiar from cosmological kinetic theory. The coefficients  $A$  and  $B$  parametrize the effective efficiency of the forward and inverse processes after averaging over phase space and macroscopic field configurations, and need not coincide despite originating from a symmetric microscopic interaction.

### IV. METHODOLOGY AND OBSERVATIONAL DATA SAMPLE

The models were analyzed employing the Markov Chain Monte Carlo (MCMC) method via the emcee package [41] to sample from our probability distribution within the  $n$ -dimensional parameter space. Observational data play a crucial role in validating cosmological models and analyzing current cosmological tensions. The precise constraints imposed by new data samples select the IDE models that best represent the observed Universe. The data samples that we will use in this work are:

- **Type Ia Supernovae (PP):** We used the Pantheon+ data [3], which consists of 1701 light curves of 1550 distinct SNe Ia, in the redshift range  $0.001 < z < 2.26$ .
- **Cosmic Chronometers (CCs):** In terms of redshift, the Hubble function,  $H(z)$ , can be expressed as  $H(z) = -\frac{1}{1+z} \frac{dz}{dt}$ . We used the most recent sample of CC data are the 32 astrophysical measurements of  $H(z)$  with covariance, obtained by estimating the differential ages of galaxies [4], in the redshift range  $0.07 < z < 1.97$ .
- **Prior From CMB (PCMB):** We employ the distance priors provided by the Planck 18 collaboration [2]. As discussed in [38], CMB distance priors

provide a good fit for cosmological models without the need to use perturbation theory to study the entire CMB power spectrum. In our analyses, we use the priors on  $\Omega_{b0}h^2$ , the shift parameter  $R$  and acoustic scale  $\ell_A$ , both defined in [38].

- **Baryon Acoustic Oscillation (BAO):** We utilize the most recent sample of BAO measurements from the DESI collaboration DR2 [37], containing measurements of  $D_M/r_{s,drag}$ ,  $D_H/r_{s,drag}$  and  $D_V/r_{s,drag}$  [42] covering the redshift range  $0.2950 < z < 2.33$ .

## V. RESULTS

To assess the viability of the proposed IDE model, we constrain its free parameters using the observational datasets and statistical framework discussed in Section IV. We perform a Bayesian analysis, sampling the posterior probability distributions of the free parameters for each observational dataset individually (PP, CCs, BAO, PCMB) and in various combinations.

We adopt wide, flat priors for the standard cosmological parameters ( $\Omega_{DM0}, \Omega_{b0}, w, H_0$ ). Regarding the interaction rate coefficients, given the lack of prior knowledge about their expected magnitude, we adopt a non-informative Jeffreys Prior (or log-uniform prior). This choice ensures scale invariance, effectively assigning equal prior probability to each order of magnitude. Consequently, we sample the exponents  $A$  and  $B$  from a uniform distribution, such that the physical interaction rates are given by  $10^A$  and  $10^B$ . The complete set of priors is summarized in Table I.

TABLE I. Priors on the free parameters of the IDE model.

Parameter	Prior Range
$\Omega_{DM0}$	[0, 1.0]
$\Omega_{b0}$	[0.01, 0.05]
$w$	[-2.0, -0.1]
$\log_{10} A$	[-60, 5]
$\log_{10} B$	[-60, 5]
$H_0$ [km s <sup>-1</sup> Mpc <sup>-1</sup> ]	[20, 120]

The marginalized constraints for the parameters  $H_0$ ,  $\Omega_{DM0}$ ,  $\Omega_{b0}$ ,  $w$ ,  $\ell_A$ , and  $r_{s,drag}$  are presented in Table II at 68% confidence level (CL). For the interaction coefficients  $\log_{10} A$  and  $\log_{10} B$ , the reported values correspond to the upper limits at 95% CL. We also display the  $1\sigma$  and  $2\sigma$  confidence contours for the full combination of data in Figure 1.

First, we analyze the constraints obtained from each dataset individually. This step is crucial to check for internal consistency among the different cosmological probes within the framework of our IDE model.

Looking at the Hubble constant,  $H_0$ , we observe a remarkable compatibility across all individual probes. The PP yield  $H_0 = 67.3 \pm 7.2$  km s<sup>-1</sup> Mpc<sup>-1</sup>, while CCs

and BAO prefer  $67.5^{+5.6}_{-6.3}$  and  $67.0^{+4.7}_{-6.7}$  km s<sup>-1</sup> Mpc<sup>-1</sup>, respectively. These values are in excellent agreement with the constraints imposed by the PCMB, which give  $H_0 = 67.7^{+2.8}_{-5.0}$  km s<sup>-1</sup> Mpc<sup>-1</sup>. It is worth noting that, within the large error bars inherent to individual late-time probes, no tension is observed. The interaction model accommodates the data with a value of  $H_0$  consistently centered around  $\sim 67$  km s<sup>-1</sup> Mpc<sup>-1</sup>.

Regarding the interaction sector, we find that the interaction parameters are constrained only as upper limits. For the individual datasets, we obtain upper limits for the annihilation exponent  $A$  ranging from  $< 5.128 \times 10^{-23}$  (PP) to  $< 6.606 \times 10^{-26}$  (CCs). The creation exponent  $\log_{10} B$  is similarly constrained, with limits ranging from  $< 3.548$  (CCs) to  $< 0.071$  (PCMB).

For the full combination (PP + PCMB + BAO + CCs), we obtain a precise measurement of the Hubble constant,  $H_0 = 67.71 \pm 0.65$  km s<sup>-1</sup> Mpc<sup>-1</sup>. Regarding the interaction parameters in the joint analysis, we find strict upper limits of  $\log_{10} A < 7.586 \times 10^{-25}$  and  $\log_{10} B < 0.048$  at 95% confidence level.

To evaluate the goodness of fit, we calculate the reduced chi-squared  $\chi^2_\nu$  [43]. For the full combination, we find  $\chi^2_\nu = 0.8889$ . For comparison, the standard flat  $\Lambda$ CDM model yields  $\chi^2_{\nu, \text{FACDM}} = 0.8796$ . Additional  $\chi^2_\nu$  values are presented in Appendix A.

We also investigate the impact of the interaction on the acoustic angular,  $\ell_A$ , and the comoving sound horizon at the drag epoch,  $r_{s,drag}$ . We observe that the interaction strength is correlated with the sound horizon. As seen in the right panel of Figure 1 and Table II, the individual background probes (PP and BAO) allow for larger values of  $r_{s,drag}$  compared to the PCMB constraint. Physically, an increase in the interaction term tends to allow for variations in  $r_{s,drag}$ . Consequently, to preserve the  $\ell_A$  consistent with observations, a decrease in  $\ell_A$  is typically observed in models with larger  $r_s$ . However, in the joint analysis, the high precision of the CMB priors dominates, fixing  $r_{s,drag} \approx 147.7$  Mpc and constraining the interaction to the small values reported above.

## VI. CONCLUSION

In this work, we have explored a new avenue within dark sector physics to address the open questions of the standard  $\Lambda$ CDM model. Unlike the “top-down” phenomenological approaches prevalent in the literature—where the interaction term is often assumed to be proportional to the Hubble parameter ( $Q \propto H\rho$ ) based merely on dimensional analysis—we have proposed a “bottom-up” model grounded in microphysics. By drawing an analogy with the Boltzmann collision term, we formulated an interaction  $Q = -A \frac{H_0}{\bar{\rho}_{c,0}} \bar{\rho}_{\text{DM}}^2 + B \frac{H_0}{\bar{\rho}_{c,0}} \bar{\rho}_{\text{DE}}^2$  that describes a reversible process of particle annihilation and creation. This formulation provides a clear physical interpretation for the coupling coefficients as thermally-averaged cross-sections per unit mass and avoids the

TABLE II. Observational constraints on the free parameters and derived quantities at 68% confidence level. Note that for the parameters  $A$  and  $B$ , the values represent the 95% confidence level upper limits (Top 5% Max) obtained in each sample.

Dataset	$H_0$	$\Omega_{DM0}$	$\Omega_{b0}$	$w$	$A$	$B$	$\ell_A$	$r_{s,drag}$
PP	$67.3 \pm 7.2$	$0.236^{+0.071}_{-0.063}$	$0.0489 \pm 0.0052$	$-0.90^{+0.17}_{-0.10}$	$< 10^{-22.29}$	$< 10^{-0.05}$	$305.2^{+9.9}_{-17}$	$153^{+15}_{-17}$
CCs	$67.5^{+5.6}_{-6.3}$	$0.279^{+0.064}_{-0.074}$	$0.0490 \pm 0.0052$	$-1.12^{+0.50}_{-0.27}$	$< 10^{-25.18}$	$< 10^{+0.55}$	$301.4^{+5.8}_{-6.8}$	$146.6^{+6.5}_{-11}$
BAO	$67.0^{+4.7}_{-6.7}$	$0.248 \pm 0.011$	$0.0498^{+0.0071}_{-0.0039}$	$-0.922 \pm 0.072$	$< 10^{-23.45}$	$< 10^{-0.81}$	$303.8^{+4.7}_{-7.0}$	$150 \pm 11$
PCMB	$67.7^{+2.8}_{-5.0}$	$0.266 \pm 0.029$	$0.0491 \pm 0.0052$	$-1.01^{+0.17}_{-0.096}$	$< 10^{-22.82}$	$< 10^{-1.15}$	$301.472 \pm 0.090$	$146.82^{+0.26}_{-0.36}$
PP + CCs	$67.7 \pm 3.6$	$0.253^{+0.055}_{-0.047}$	$0.0490 \pm 0.0052$	$-0.93^{+0.13}_{-0.10}$	$< 10^{-23.07}$	$< 10^{-0.10}$	$301.2^{+5.0}_{-6.2}$	$148.9^{+6.3}_{-7.8}$
BAO + PCMB	$69.0 \pm 1.1$	$0.2495^{+0.0063}_{-0.0074}$	$0.0473 \pm 0.0015$	$-1.017 \pm 0.045$	$< 10^{-23.97}$	$< 10^{-1.31}$	$301.401 \pm 0.088$	$147.36^{+0.18}_{-0.42}$
PP + BAO + CCs	$67.4 \pm 2.9$	$0.2475^{+0.0097}_{-0.011}$	$0.0513^{+0.0053}_{-0.0028}$	$-0.916 \pm 0.037$	$< 10^{-23.59}$	$< 10^{-0.73}$	$302.8^{+2.8}_{-3.4}$	$148.2^{+5.6}_{-6.7}$
PP + PCMB + CCs	$66.53 \pm 0.82$	$0.2735 \pm 0.0083$	$0.0505 \pm 0.0012$	$-0.971 \pm 0.031$	$< 10^{-24.38}$	$< 10^{-1.25}$	$301.470 \pm 0.090$	$146.83^{+0.26}_{-0.35}$
PP + PCMB + BAO + CCs	$67.71 \pm 0.65$	$0.2575^{+0.0047}_{-0.0052}$	$0.04907 \pm 0.00091$	$-0.963 \pm 0.028$	$< 10^{-24.12}$	$< 10^{-1.32}$	$301.406^{+0.092}_{-0.10}$	$147.72^{+0.48}_{-0.64}$

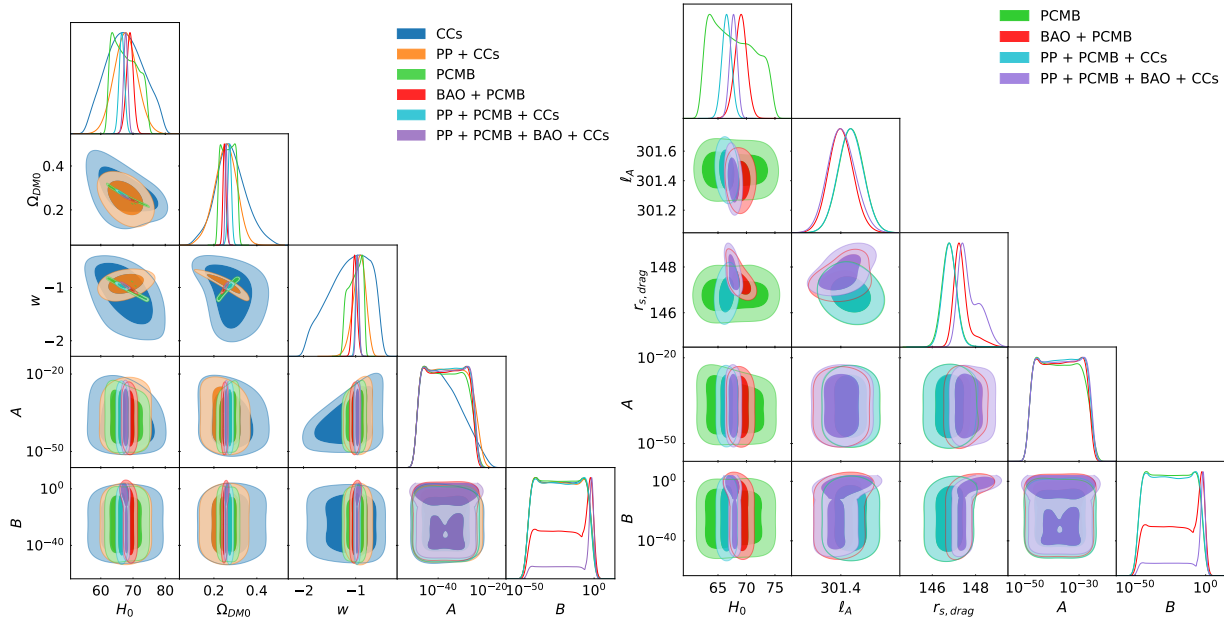


FIG. 1. Marginalized  $1\sigma$  and  $2\sigma$  confidence contours and posterior distributions for the free parameters. **Left:** Constraints on the primary model parameters:  $H_0$ ,  $\Omega_{DM0}$ ,  $w$ , and the interaction exponents  $A$ ,  $B$ . **Right:** Constraints highlighting the derived acoustic scales:  $H_0$ ,  $\ell_A$ ,  $r_{s,drag}$ , alongside the interaction exponents  $A$ ,  $B$ . Note that for clarity, not all individual dataset combinations are shown in every panel.

theoretical issues of non-locality associated with  $H$ -dependent interactions.

The constraints on the Hubble constant obtained from individual datasets are remarkably consistent with each other within the framework of our model. The combined analysis yields a precise measurement of  $H_0 = 67.71 \pm 0.65 \text{ km s}^{-1} \text{ Mpc}^{-1}$ . A crucial finding of our analysis is the stringent constraint on the interaction strength. Contrary to models that require significant coupling to fit the data, we found strict upper limits for both interaction coefficients at the 95% confidence level. For the combined dataset, the interaction coefficient  $A$  is constrained to  $A < 7.586 \times 10^{-25}$ , while the coefficient  $B$  is limited to  $B < 0.048$  at 95% CL. Crucially, the combination of these limits with the observational bound on  $H_0$  translates directly into a constraint on the thermally-averaged annihilation cross-section per unit of mass. Due to the cosmic expansion rate and the vast characteristic

size of the Universe, the measured cross-section today appears as a small, yet non-null value, which stimulates the search for more precise limits using complementary data sources.

We also performed a model selection analysis using the reduced chi-squared statistic. We found that the IDE model yields  $\chi^2_\nu \approx 0.88$ , a value highly comparable to that of the standard  $\Lambda$ CDM model (0.8796). This demonstrates that the proposed IDE scenario is a viable cosmological model that fits the observational data with high precision.

Finally, we observed a correlation between the interaction strength and the comoving sound horizon at the drag epoch,  $r_{s,drag}$ . While individual background probes allow for larger deviations in  $r_{s,drag}$ , the inclusion of CMB priors breaks this degeneracy, fixing the sound horizon to  $\approx 147.7 \text{ Mpc}$  and consequently suppressing the allowed interaction range. Future perspectives for this work in-

clude extending the analysis to linear perturbations to investigate if the microphysical nature of this coupling affects the growth of structure ( $f\sigma_8$ ) and the full CMB power spectrum distinctively from standard  $\Lambda$ CDM.

## ACKNOWLEDGMENTS

AAE and FBA acknowledge the support from the University of Science and Technology of China. FBA also acknowledge support from the Chinese Academy of Sciences as well as the Br-A Talent Program.

## Appendix A: Details of the Statistical Analysis

We observe in Figure (1) that when combining the BAO+PCMB datasets, either alone or with other data samples, the distribution for the parameter  $B$  exhibits a plateau followed by a sharp peak at the right edge of the sample range. To improve visualization, we produced two types of plots: first, we plotted the frequency versus  $\ln \mathcal{L}$ , and second,  $\ln \mathcal{L}$  versus  $\log_{10} B$ . These are presented in Figures (2) and (3).

In Figure (2), we present the plots for the combined dataset of PP, PCMB, BAO, and CCs. In the left panel, displaying frequency versus  $\ln \mathcal{L}$ , we observe that the distribution possesses two peaks, characterizing a bimodal distribution. We notice that the most frequent peak, around  $\ln \mathcal{L} \approx -719$ , is close to the distribution's median; however, it does not represent the maximum likelihood value (best fit) of  $\ln \mathcal{L} \approx -715$ , which is found in the second peak. The right panel illustrates the manifestation of this second peak in the relationship between  $\ln \mathcal{L}$  and  $\log_{10} B$ , where we observe a sharp tip at the end of the sample. The same discussion extends to Figure (3), where we present similar plots but specifically for the analysis of PCMB+BAO. In this case, we observe that the second peak is less populated compared to the

second peak in Figure (2).

We calculated the reduced chi-squared value,  $\chi^2_\nu$ , for each data sample analyzed for the proposed IDE model and for the standard model. The values are listed in Table (III). We observe that for the full combination of datasets (PP + PCMB + BAO + CCs), the Interaction Dark Energy (IDE) model yields a  $\chi^2_\nu$  of 0.8805, which is highly comparable to the value obtained for the  $\Lambda$ CDM model (0.8796). This suggests that the IDE model provides a statistical fit of similar quality to the standard model when all data sets are considered simultaneously. However, when analyzing the datasets individually, distinct behaviors emerge. For the BAO dataset alone, the IDE model presents a significantly higher reduced chi-squared value (1.5050) compared to  $\Lambda$ CDM (1.1426), indicating a tension between the IDE model and the BAO data. This tension persists in the BAO+PCMB combination, where the IDE model again shows a poorer fit (1.7362) compared to the standard model (1.3379).

TABLE III.  $\chi^2_\nu$  of each data sample for the IDE model and for the  $\Lambda$ CDM model.

Data	$\chi^2_\nu, \text{IDE}$	$\chi^2_\nu, \text{FACDM}$
PP	0.8860	0.8847
CCs	0.5743	0.5190
BAO	1.5050	1.1426
PCMB	-	-
PP + CCs	0.8776	0.8762
BAO+PCMB	1.7362	1.3379
PP + PCMB + CCs	0.8761	0.8750
PP + BAO+ CCs	0.8761	0.8775
PP + PCMB + BAO + CCs	0.8805	0.8796

Conversely, for the PP and CCs datasets, both individually and in combination, the performance of the IDE model is nearly identical to that of  $\Lambda$ CDM, with  $\chi^2_\nu$  values remaining well below unity, indicating a good fit to these specific observations.

---

[1] R. L. Workman *et al.* (Particle Data Group), Review of Particle Physics, PTEP **2022**, 083C01 (2022).

[2] N. Aghanim *et al.* (Planck), Planck 2018 results. VI. Cosmological parameters, Astron. Astrophys. **641**, A6 (2020), [Erratum: Astron. Astrophys. 652, C4 (2021)], arXiv:1807.06209 [astro-ph.CO].

[3] D. Brout *et al.*, The Pantheon+ Analysis: Cosmological Constraints, Astrophys. J. **938**, 110 (2022), arXiv:2202.04077 [astro-ph.CO].

[4] M. Moresco *et al.*, Unveiling the Universe with emerging cosmological probes, Living Rev. Rel. **25**, 6 (2022), arXiv:2201.07241 [astro-ph.CO].

[5] E. Abdalla *et al.*, Cosmology intertwined: A review of the particle physics, astrophysics, and cosmology associated with the cosmological tensions and anomalies, JHEAp **34**, 49 (2022), arXiv:2203.06142 [astro-ph.CO].

[6] L. Perivolaropoulos and F. Skara, Challenges for  $\Lambda$ CDM: An update, New Astron. Rev. **95**, 101659 (2022), arXiv:2105.05208 [astro-ph.CO].

[7] L. S. Brito, J. F. Jesus, A. A. Escobal, and S. H. Pereira, Can decaying vacuum solve the  $H_0$  tension?, Eur. Phys. J. C **85**, 1025 (2025), arXiv:2412.06756 [astro-ph.CO].

[8] J. A. S. Lima, Alternative dark energy models: An Overview, Braz. J. Phys. **34**, 194 (2004), arXiv:astro-ph/0402109.

[9] M. B. Gavela, L. Lopez Honorez, O. Mena, and S. Rigolin, Dark Coupling and Gauge Invariance, JCAP **11**, 044, arXiv:1005.0295 [astro-ph.CO].

[10] G. R. Farrar and P. J. E. Peebles, Interacting dark matter and dark energy, Astrophys. J. **604**, 1 (2004), arXiv:astro-ph/0307316.

[11] R. von Marttens, V. Marra, L. Casarini, J. E. Gonzalez, and J. Alcaniz, Null test for interactions in the dark sector, Phys. Rev. D **99**, 043521 (2019), arXiv:1812.02333

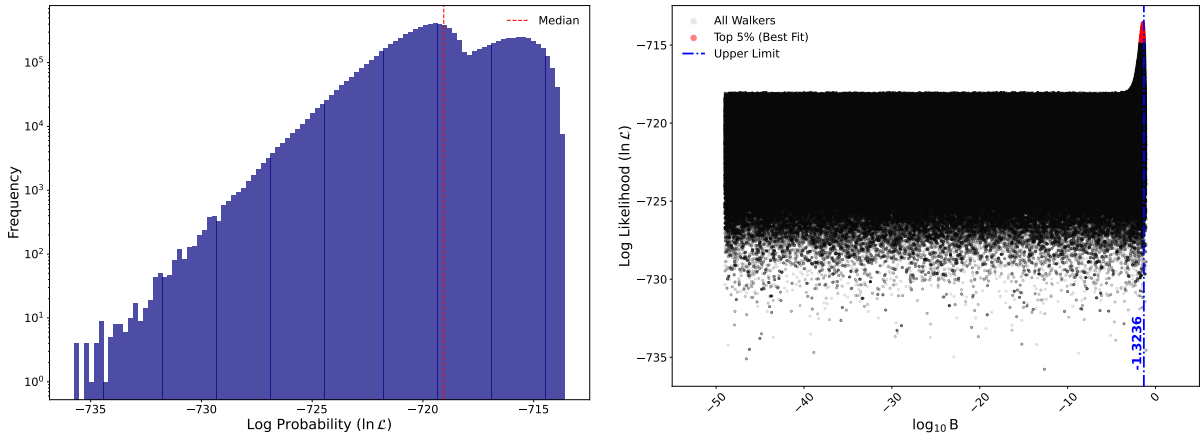


FIG. 2. PP + PCMB + BAO + CCs. **Left:** Frequency  $\times \ln \mathcal{L}$ . **Right:**  $\ln \mathcal{L} \times \log_{10} B$ .

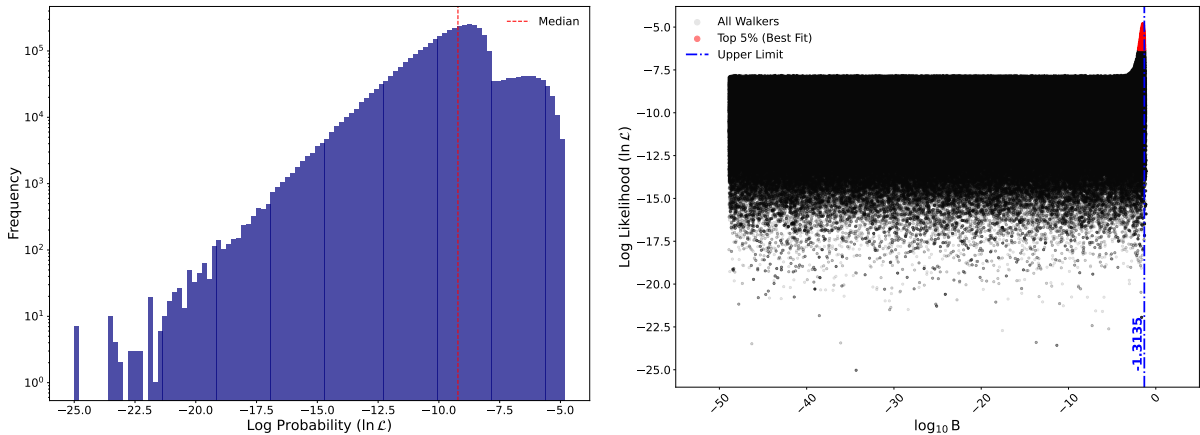


FIG. 3. BAO + PCMB. **Left:** Frequency  $\times \ln \mathcal{L}$ . **Right:**  $\ln \mathcal{L} \times \log_{10} B$ .

[astro-ph.CO].

[12] V. Salvatelli, N. Said, M. Bruni, A. Melchiorri, and D. Wands, Indications of a late-time interaction in the dark sector, *Phys. Rev. Lett.* **113**, 181301 (2014), arXiv:1406.7297 [astro-ph.CO].

[13] A. Shafieloo, D. K. Hazra, V. Sahni, and A. A. Starobinsky, Metastable Dark Energy with Radioactive-like Decay, *Mon. Not. Roy. Astron. Soc.* **473**, 2760 (2018), arXiv:1610.05192 [astro-ph.CO].

[14] R. J. F. Marcondes, R. C. G. Landim, A. A. Costa, B. Wang, and E. Abdalla, Analytic study of the effect of dark energy-dark matter interaction on the growth of structures, *JCAP* **12**, 009, arXiv:1605.05264 [astro-ph.CO].

[15] B. Wang, E. Abdalla, F. Atrio-Barandela, and D. Pavon, Dark Matter and Dark Energy Interactions: Theoretical Challenges, Cosmological Implications and Observational Signatures, *Rept. Prog. Phys.* **79**, 096901 (2016), arXiv:1603.08299 [astro-ph.CO].

[16] R. F. vom Marttens, L. Casarini, W. S. Hipólito-Ricaldi, and W. Zimdahl, CMB and matter power spectra with non-linear dark-sector interactions, *JCAP* **01**, 050, arXiv:1610.01665 [astro-ph.CO].

[17] L. Santos, W. Zhao, E. G. M. Ferreira, and J. Quintin, Constraining interacting dark energy with CMB and BAO future surveys, *Phys. Rev. D* **96**, 103529 (2017), arXiv:1707.06827 [astro-ph.CO].

[18] W. Yang, S. Pan, and J. D. Barrow, Large-scale Stability and Astronomical Constraints for Coupled Dark-Energy Models, *Phys. Rev. D* **97**, 043529 (2018), arXiv:1706.04953 [astro-ph.CO].

[19] A. Cid, B. Santos, C. Pigozzo, T. Ferreira, and J. Alcaniz, Bayesian Comparison of Interacting Scenarios, *JCAP* **03**, 030, arXiv:1805.02107 [astro-ph.CO].

[20] R. G. Landim, Cosmological perturbations and dynamical analysis for interacting quintessence, *Eur. Phys. J. C* **79**, 889 (2019), arXiv:1908.03657 [gr-qc].

[21] E. Di Valentino, A. Melchiorri, O. Mena, and S. Vagnozzi, Interacting dark energy in the early 2020s: A promising solution to the  $H_0$  and cosmic shear tensions, *Phys. Dark Univ.* **30**, 100666 (2020), arXiv:1908.04281 [astro-ph.CO].

[22] J. F. Jesus, A. A. Escobal, D. Benndorf, and S. H. Pereira, Can dark matter-dark energy interaction alleviate the cosmic coincidence problem?, *Eur. Phys. J. C* **82**, 273 (2022), arXiv:2012.07494 [astro-ph.CO].

- [23] M. Lucca and D. C. Hooper, Shedding light on dark matter-dark energy interactions, *Phys. Rev. D* **102**, 123502 (2020), arXiv:2002.06127 [astro-ph.CO].
- [24] R. von Marttens, J. E. Gonzalez, J. Alcaniz, V. Marra, and L. Casarini, Model-independent reconstruction of dark sector interactions, *Phys. Rev. D* **104**, 043515 (2021), arXiv:2011.10846 [astro-ph.CO].
- [25] L. A. Anchordoqui, E. Di Valentino, S. Pan, and W. Yang, Dissecting the H0 and S8 tensions with Planck + BAO + supernova type Ia in multi-parameter cosmologies, *JHEAp* **32**, 28 (2021), arXiv:2107.13932 [astro-ph.CO].
- [26] S. Gariazzo, E. Di Valentino, O. Mena, and R. C. Nunes, Late-time interacting cosmologies and the Hubble constant tension, *Phys. Rev. D* **106**, 023530 (2022), arXiv:2111.03152 [astro-ph.CO].
- [27] R. C. Nunes, S. Vagnozzi, S. Kumar, E. Di Valentino, and O. Mena, New tests of dark sector interactions from the full-shape galaxy power spectrum, *Phys. Rev. D* **105**, 123506 (2022), arXiv:2203.08093 [astro-ph.CO].
- [28] A. Bernui, E. Di Valentino, W. Giarè, S. Kumar, and R. C. Nunes, Exploring the H0 tension and the evidence for dark sector interactions from 2D BAO measurements, *Phys. Rev. D* **107**, 103531 (2023), arXiv:2301.06097 [astro-ph.CO].
- [29] Y. Zhai, W. Giarè, C. van de Bruck, E. Di Valentino, O. Mena, and R. C. Nunes, A consistent view of interacting dark energy from multiple CMB probes, *JCAP* **07**, 032, arXiv:2303.08201 [astro-ph.CO].
- [30] G. A. Hoerning, R. G. Landim, L. O. Ponte, R. P. Rolim, F. B. Abdalla, and E. Abdalla, Constraints on interacting dark energy revisited: Implications for the Hubble tension, *Phys. Rev. D* **112**, 023523 (2025), arXiv:2308.05807 [astro-ph.CO].
- [31] B. Wang, E. Abdalla, F. Atrio-Barandela, and D. Pavón, Further understanding the interaction between dark energy and dark matter: current status and future directions, *Rept. Prog. Phys.* **87**, 036901 (2024), arXiv:2402.00819 [astro-ph.CO].
- [32] J. Valivita, E. Majerotto, and R. Maartens, Instability in interacting dark energy and dark matter fluids, *JCAP* **07**, 020, arXiv:0804.0232 [astro-ph].
- [33] J.-H. He, B. Wang, and E. Abdalla, Stability of the curvature perturbation in dark sectors' mutual interacting models, *Phys. Lett. B* **671**, 139 (2009), arXiv:0807.3471 [gr-qc].
- [34] R. von Marttens, L. Casarini, D. F. Mota, and W. Zimdahl, Cosmological constraints on parametrized interacting dark energy, *Phys. Dark Univ.* **23**, 100248 (2019), arXiv:1807.11380 [astro-ph.CO].
- [35] D. Figueruelo, M. van der Westhuizen, A. Abebe, and E. Di Valentino, Late-time Background Constraints on Linear and Non-linear Interacting Dark Energy after DESI DR2, (2026), arXiv:2601.03122 [astro-ph.CO].
- [36] E. W. Kolb and M. S. Turner, *The Early Universe*, Vol. 69 (Taylor and Francis, 2019).
- [37] M. Abdul Karim *et al.* (DESI), DESI DR2 results. II. Measurements of baryon acoustic oscillations and cosmological constraints, *Phys. Rev. D* **112**, 083515 (2025), arXiv:2503.14738 [astro-ph.CO].
- [38] L. Chen, Q.-G. Huang, and K. Wang, Distance Priors from Planck Final Release, *JCAP* **02**, 028, arXiv:1808.05724 [astro-ph.CO].
- [39] A. A. Escobal, J. F. Jesus, and S. H. Pereira, Cosmological constraints on scalar field dark matter, *Int. J. Mod. Phys. D* **30**, 2150108 (2021), arXiv:2004.06495 [astro-ph.CO].
- [40] Q. Liu, C. Feng, and F. B. Abdalla, Improved constraints on ultralight axions using latest observations of the early and late Universe, (2025), arXiv preprint, arXiv:2511.18917 [astro-ph.CO].
- [41] D. Foreman-Mackey, D. W. Hogg, D. Lang, and J. Goodman, emcee: The MCMC Hammer, *Publ. Astron. Soc. Pac.* **125**, 306 (2013), arXiv:1202.3665 [astro-ph.IM].
- [42] Let  $D_M$  be the transverse comoving distance,  $D_H$  the Hubble distance,  $D_V$  the isotropic BAO distance, and  $r_{s,drag}$  the comoving sound horizon at the drag epoch. For the calculation of the drag epoch redshift,  $z_d$ , we adopt the approximation described in [44].
- [43] Defined as:  $\chi_\nu^2 \equiv \frac{\chi_{min}^2}{n-p}$  [7].
- [44] W. Hu and N. Sugiyama, Small scale cosmological perturbations: An Analytic approach, *Astrophys. J.* **471**, 542 (1996), arXiv:astro-ph/9510117.